idine, and trimethylsilyl triflate for the Si). The methyl enol ethers were prepared by mixing the appropriate ketone (1 mol equiv), trimethyl orthoformate (1.1 equiv), and *p*-toluenesulfonic acid (0.005 equiv) at room temperature for 24 h. The methyl formate and the methanol formed were distilled slowly for at least 4 h until no more methanol was formed. The methyl enol ethers were then distilled under reduced pressure.

Physical Properties of the New Compounds. A. 1-Acetoxy-1-fluoro-2-methoxy-3,4-dihydronaphthalene (4): IR 1745 cm^{-1}; ^1H NMR 7.8–7.2 (4 H, m), 4.72 (1 H, m), 3.43 (3 H, s), 3.0 (1 H, m), 2.65 (1 H, m), 2.30 (1 H, m), 2.17 (3 H, s), 2.08 (1 H, m); ^{19}F NMR −91.64 ppm (s); ^{13}C NMR 129.8, 128.5, 127.3, 126.5 (C_{arom}), 109.4 (d, $^1J_{CF}$ = 227 Hz), 74.7 (d, $^2J_{CF}$ = 32 Hz), 57.2, 23.10, 22.6, 22.5 ppm; MS *m/z* 178 [(M − AcOH)$^+$].

B. 1-Acetoxy-1-fluoro-1-phenyl-2-methoxyethane (7): ^1H NMR 7.45–7.24 (5 H, m), 3.79 (2 H, d, *J* = 15 Hz), 3.39 (3 H, s), 2.12 (3 H, s); ^{19}F NMR −122 ppm (t, *J* = 15 Hz); ^{13}C NMR 167.3 (CO), 130–120 (C_{arom}), 111 (d, $^1J_{CF}$ = 233 Hz), 76 (d, $^2J_{CF}$ = 30 Hz), 59.9, 21.67 ppm. Anal. Calcd for $C_{11}H_{13}FO_3$: C, 62.26; H, 6.13. Found: C, 62.10; H, 6.25.

C. 1-Phenyl-1,1,2-trimethoxyethane (15): ^1H NMR 7.98–7.26 (5 H, m), 3.64 (2 H, s), 3.23 (6 H, s), 3.2 (3 H, s); MS *m/z* 165 [(M − OMe)$^+$], 151 [(M − CH_2OMe)$^+$].

D. 1,1,2-Trimethoxy-4-*tert*-butylcyclohexane (16): ^1H NMR 3.44–3.38 (1 H, m), 3.35 (3 H, s), 3.2 (3 H, s), 3.17 (3 H, s), 2.2–1.8 (2 H, m), 1.6–1.2 (5 H, m), 0.9 (9 H, s); ^{13}C NMR 100.05, 76.31, 55.75, 47.37, 46.93, 39.9, 31.6, 27.35, 27.62, 25.5, 22.5 ppm; MS *m/z* 199 [(M − OMe)$^+$], 173 [(M − *t*-Bu)$^+$], 57 [(*t*-Bu)$^+$].

E. 4-Methoxy-5-nonanone (18): IR 1710 cm^{-1}; ^1H NMR 3.58 (1 H, t, *J* = 6.2 Hz), 3.37 (3 H, s), 2.52 (2 H, t, *J* = 7.2 Hz); MS *m/z* 87 [PrCHOMe]$^+$, 85 [BuCO]$^+$, 57 [Bu]$^+$. Anal. Calcd for $C_{10}H_{20}O_2$: C, 69.76; H, 11.6. Found: C, 69.53; H, 11.2.

Acknowledgment. This research was supported by Grant No. 89-00079 from the USA–Israel Binational Science Foundation (BSF), Jerusalem, Israel.

Synthesis and Study of New α-Haloacid Ferroelectric Liquid Crystal Derivatives. MM2 Approach to the Molecular Structure–Ferroelectric Activity Relationship

T. Sierra,† J. L. Serrano,*,† M. B. Ros,† A. Ezcurra,‡ and J. Zubía§

Contribution from the Química Orgánica, Facultad de Ciencias, Instituto de Ciencia de Materiales de Aragón, Universidad de Zaragoza-C.S.I.C., 50009-Zaragoza, Spain, Departamento de Física Aplicada II, Facultad de Ciencias, Universidad del País Vasco, Aptdo 644, 48080-Bilbao, Spain, and Departamento de Automática, Electronica y Telecomunicaciones, Escuela Técnica Superior de Ingenieros Industriales y de Telecomunicación, Universidad del País Vasco, Alameda de Urquijo s/n, 48013-Bilbao, Spain. *Received December 31, 1991*

Abstract: In order to understand the structural factors that influence ferroelectric properties, three new series (**F**, **Cl**, and **Br**) of chiral naphthalene-ring derived compounds were synthesized, and their ferroelectric properties [spontaneous polarization (Ps) and response time (τ)] were evaluated in the pure compound. The chiral tails are α-halo acids derived from L-α-amino acids: L-α-alanine (**1**), L-leucine (**2**), L-isoleucine (**3**), and L-valine (**4**), with a fluorine, chlorine, or bromine atom in the chiral center. The highest Ps values were obtained for compounds containing a fluorine or chlorine atom in their asymmetric center and with chiral tail derived from L-isoleucine (**3**) (**F-3**, 102 nC/cm^2; **Cl-3**, 100 nC/cm^2). The steric requirements of the halogen atom and the bulky alkyl group in the asymmetric center determine the most stable conformations of these chiral tails, which have been studied by molecular mechanic empirical calculations, MM2. MM2 calculations prove to be a successful tool for understanding how the structure of the lateral chiral tail affects molecular arrangement and, as a consequence, the ferroelectric properties of the materials.

Introduction

Since the discovery, in 1975, of the first ferroelectric liquid crystal, DOBAMBC,[1] considerable efforts have been made to design and synthesize new organic molecules with structures that will give rise to SmC* arrangement and good ferroelectric properties.[2,3] The study of the relationship between molecular structure and ferroelectric activity has been one of the most interesting subjects,[2-4] and, as a consequence, the challenge of finding a model which reflects this relationship has been the aim of many researchers. In 1986, Walba et al.[5] proposed a model, the "Boulder Model", for the molecular origins of the spontaneous polarization, which has been successfully applied to the design of new FLC materials with high Ps values.[6] In 1990, Koden et al.[7] published a model, based on the "zigzag" model for the smectic C phase, which has been used to investigate the spontaneous polarization of some chiral compounds possessing cis and trans isomers.[8] Both models are mainly based on the disposition of the chiral tail in the SmC* phase.

Chart I

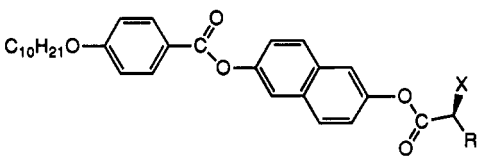

	-R	
1	-CH_3	X = F, Cl, Br
2	-$CH_2CH(CH_3)_2$	
3	-*$CH(CH_3)CH_2CH_3$	
4	-$CH(CH_3)_2$	

In this paper, we have tried to approach this subject from a different viewpoint: molecular mechanic empirical calculations[9]

* Corresponding author.
† University of Zaragoza.
‡ F.C., Universidad del País Vasco.
§ E.T.S.I.I.T., Universidad del País Vasco.

(1) Meyer, R. B.; Liébert, L.; Strzelecki, L.; Keller, P. *J. Physique (Lett.)* **1975**, *36*, L-69.

0002-7863/92/1514-7645$03.00/0

are a useful tool to study the different conformations of the chiral tails in a FLC molecule. These calculations can help us to understand how structural factors concerning the chiral tails affect ferroelectric behavior.

In a previous paper,[10] we presented three series of Schiff bases whose chiral tails were α-chloro acids and β-chlorohydrines derived from L-α-amino acids (L-α-alanine, L-leucine, L-isoleucine, and L-valine). In the paper, our results suggested that the presence of a carbonyl group adjacent to the asymmetric carbon increased the Ps values. However, these Schiff bases containing α-chloro esters did not show the high chemical stability desired in FLC materials.

The present paper deals with three new series of compounds containing 6-(2-hydroxy)naphthyl benzoate as a chemically stable core. The chiral tails are α-amino acid derivatives where the amino group has been substituted by fluorine, chlorine, and bromine atoms (see Chart I).

In these compounds, the molecular arrangement is likely to be affected by the alkyl group in the chiral tail as well as the halogen atom in the asymmetric center. This halogen atom is going to contribute to the molecular arrangement, and consequently to the ferroelectric properties, in two ways: firstly, bringing a strong dipole moment to the molecule in its asymmetric part and, secondly, affecting the conformations of the chiral tail because of its steric requirements.

Bearing this in mind, we consider that the study of these factors through empirical calculations might be greatly helpful in understanding the relationship between molecular structure and ferroelectric properties in terms of the intra- and intermolecular coupling of the dipoles, which would help us to obtain theoretical models that could be applied to the design of new molecules for ferroelectric liquid crystals.

We report herein, detailed results of the synthetic process, and the evaluation of the mesogenic and ferroelectric properties of these three series of compounds as well as an exhaustive study of their chiral tails through molecular mechanic empirical calculations (MM2).

For the sake of simplification, each compound is named by the chemical symbol of the halogen in its chiral center (**F, Cl, Br**) and an arabic (**1–4**) number corresponding to the series and terminal tail, respectively.

Results and Discussion

Synthesis. The full synthetic scheme is outlined in Scheme I.

The chiral tails introduced in these compounds were all prepared from the corresponding commercial L-α-amino acids [**1**] readily available in high enantiomeric purity: L-α-alanine, L-leucine, L-isoleucine, and L-valine. The α-halo acids [**2**] were synthesized by means of a nucleophilic substitution of the amino group by the halogen atom via the diazonium salt. When the halogen atom was chlorine or bromine, the reaction medium (**A**) was 6 N HCl and 6 N HBr, respectively, as reported by Fu et al.[11] For the fluorine derivatives, the reaction medium was a solution of HF in pyridine [70/30] using the method described by Olah.[12] When L-isoleucine and L-valine were the substrates, it was necessary to use a less acidic reaction medium (HF/Py [48/52]) in order to avoid the formation of mixtures of fluoro acids as a consequence of anchimerically assisted rearrangements of the groups linked to the chiral center.[13,14] In all cases the nucleophilic substitution takes place with retention of the asymmetric center configuration.[15]

Scheme I

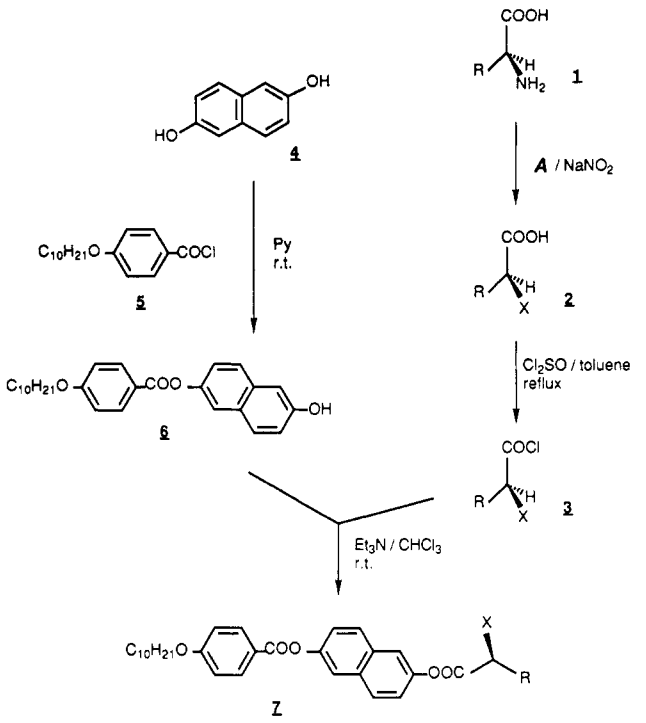

Starting from commercial 2,6-dihydroxynaphthalene, the mesogenic nucleus can be easily prepared. Esterification of this material with 4-decyloxybenzoyl chloride [**5**]—previously obtained by refluxing the corresponding 4-decyloxybenzoic acid in Cl_2SO and DMF as a catalyst—in pyridine affords a 40% yield of the monoester [**6**].

The coupling of the intermediate **6** with the corresponding α-halo acids was carried out by esterification with the α-haloacyl chloride previously prepared by refluxing the starting α-halo acid in Cl_2SO. This reaction gives rise to the enantiomerically pure α-halo esters derivatives [**7**] unlike the esterification method which uses DCC/DMAP as esterification reagents.[16] A study of the isoleucine derivatives prepared by both methods through ^1H NMR spectroscopy showed that when DCC is used, partial racemization is produced in the final compound when Cl or Br is present in the chiral center. The presence of the second asymmetric carbon in the molecule gives rise to two diastereomeric compounds when there is a mixture of the *R* and *S* enantiomers in the asymmetric carbon with the halogen atom. When DCC was used with α-chloro acids and α-bromo acids, two signals were observed for the hydrogen belonging to this carbon atom. None of the isoleucine derivatives prepared via acid chloride showed peaks due to the presence of diastereoisomers. We have assumed that since

(2) Lagerwall, S. T.; Otterholm, B.; Skarp, K. *Mol. Cryst. Liq. Cryst.* **1987**, *152*, 503.
(3) Beresnev, L. A.; Blinov, L. M.; Osipov, M. A.; Pikin, S. A. *Mol. Cryst. Liq. Cryst.* **1988**, *158A*, 3.
(4) Walba, D. M. Ferroelectric Liquid Crystals. A Unique State of Matter. In *Advances in the Synthesis and Reactivity of Solids*; Mallouk, T. E., Ed.; JAI Press Ltd.: Greenwich, CT, 1991; Vol. 1, p 173.
(5) Walba, D. M.; Slater, S. C.; Thurmes, W. N.; Clark, N. A.; Handshy, M. A.; Supon, F. *J. Am. Chem. Soc.* **1986**, *108*, 5210.
(6) (a) Walba, D. M.; Clark, N. A. *Proc. SPIE* **1987**, *825*, 81. (b) Walba, D. M.; Clark, N. A. *Ferroelectrics* **1988**, *84*, 65. (c) Walba, D. M.; Razavi, H. A.; Horiuchi, A.; Eidman, K. F.; Otterholm, B.; Haltiwanger, R. C.; Clark, N. A.; Shao, R.; Parmar, D. S.; Wand, M. D.; Vohra, R. T. *Ferroelectrics* **1991**, *113*, 21.
(7) Koden, M.; Kuratate, T.; Funada, F.; Awane, K.; Sakaguchi, K.; Shiomi, Y. *Mol. Cryst. Liq. Cryst. Lett.* **1990**, *7*, 79.
(8) (a) Koden, M. *Third International Conference on Ferroelectric Liquid Crystals*; June 24–28, 1991, Boulder, Colorado, USA, O–17. (b) Koden, M.; Shiomi, Y.; Nakagawa, K.; Funada, F.; Awana, K.; Yamazaki, T.; Kitazume, T. *Jpn. J. Appl. Phys.* **1991**, *30*, 1300.
(9) Allinger, N. L. *J. Am. Chem. Soc.* **1977**, *9*, 8127.
(10) Sierra, T.; Melĕndez, E.; Serrano, J. L.; Ezcurra, A.; Pérez-Jubindo, M. A. *Chem. Mat.* **1991**, *3*, 157.
(11) Fu, S. C. J.; Birnbaum, S. M.; Greenslein, I. P. *J. Am. Chem. Soc.* **1954**, *76*, 6054.
(12) Olah, G. A.; Welch, J. T. *Synthesis* **1974**, 652.
(13) Olah, G. A.; Surya Prakash, G. K.; Chao, Y. L. *Helv. Chim. Acta* **1981**, *64*, 2528.
(14) Barber, J.; Keck, R.; Retey, J. *Tetrahedron Lett.* **1982**, *23*, 1549.
(15) Faustini, F.; Demunari, S.; Panzevi, A.; Villa, V.; Gandolfi, C. A. *Tetrahedron Lett.* **1981**, *22*, 4533.
(16) (a) Sakurai, T.; Mikami, N.; Higuchi, R.; Honma, M.; Ozaki, M.; Yoshino, K. *J. Chem. Soc., Chem. Commun.* **1986**, 978. (b) Yoshino, K.; Ozaki, M; Kishio, S.; Sakurai, T.; Mikami, N.; Higuchi, R.; Honma, M. *Mol. Cryst. Liq. Cryst.* **1987**, *144*, 87.

Table I. Transition Temperatures (°C) for the Compounds in Series F, Cl, and Br in the Second Heating and Cooling Processes

compd	C		S_C*		S_A		Ch		I
F-1	●	110.5	(S_B	94.1)[c]	●	129.5	●	147.3	●
F-2	●	78.0	(●	77.0)[a]	●	119.8			●
F-3	●	79.3	(●	78.0)[a]	●	103.3	●	109.8	●
F-4	●	86.7	(●	85.0)[a]	●	117.2	●	132.1	●
Cl-1	●	92.4			●	122.4	●	131.7	●
Cl-2	●	77.9	(●	71.2)[a]	●	96.4			●
Cl-3	●	68.1	●	75.0[a]	●	95.2	●	99.5	●
Cl-4	●	62.7	●	86.8[a]	●	104.7	●	111.8	●
Br-1	●	92.5	(●	86.5)[a]	●	108.5	●	123.1	●
Br-2	●	70.7	(●	68.5)[a,b]	●	84.9			●
Br-3	●	74.8	●	77.5[a]	●	86.5	●	97.4	●
Br-4	●	64.1	●	82.1[a]	●	92.1	●	104.8	●

[a] Optical microscopy data. [b] Enantiotropic SmC* phase in the first scan in DSC. [c] ( ) Monotropic transition.

the synthetic process is the same, all the compounds behave similarly as far as optical purity is concerned.

Mesophase Characterization. The mesophases were identified according to their textures which were observed by optical microscopy.

In the heating process the SmC* appears from the crystal in a blurred-Schlieren texture, which gives rise to Schlieren and homeotropic coexistent textures in the SmA. In the cooling process, the SmA mesophase appears from the Ch mesophase, in a focal-conic texture which remains in the SmC*. Dechiralization lines were observed in the ferroelectric mesophase for some of the compounds. Marbled and pseudohomeotropic textures in the SmC* can be obtained when the focal-conic texture is mechanically stressed.

From the isotropic liquid, the Ch phase appears as a focal-conic texture showing the typical fingerprints. When mechanically stressed, oily streak, and cell textures appear. These textures give rise to iridescence when they are observed by white light, due to the interaction of the light with the helicoidal structure.[17]

The orthogonal mesophase SmB in compound **F-1** was identified by its mosaic and homeotropic textures, which appear from focal-conic and homeotropic textures of the SmA phase on cooling.

Mesogenic Properties. The thermal data of the compounds of the three series are gathered in Table I.

All the compounds, except **F-1** and **Cl-1**, show the potentially ferroelectric SmC* mesophase.

None of the compounds in series **F**, with a fluorine atom in the chiral center, shows a thermodynamically stable SmC* phase. All of them enter a SmA phase on heating the crystalline solid. Three of them, **F-2**, **F-3**, and **F-4**, exhibit a monotropic SmC* phase as shown in Figure 1.

The stability of the SmC* phase increases in the compounds of series **Cl** and **Br**. The compounds whose chiral tails are L-isoleucine and L-valine derivatives (**Cl-3** and **Cl-4** and **Br-3** and **Br-4**) show an enantiotropic SmC* phase in both series.

With regard to the liquid crystal state stability, the widest ranges are found in series **F**, with orthogonal behavior always favored (SmA and SmB in compound **F-1**). In the compounds of series **Br**, the bromine atom seems to destabilize the mesomorphic state affecting, especially, the SmA phase.

Interestingly, a cholesteric phase appears above the SmA phase in all the compounds derived from L-α-alanine, L-isoleucine, and L-valine amino acids. This gives rise to the sequence I → Ch → SmA → SmC* which favors the homogeneous alignment of the molecules in the cell, allowing a more accurate measurement of the ferroelectric properties.[18,19]

Ferroelectric Properties. Experimental Data. The ferroelectric properties, spontaneous polarization (Ps) and response times (τ), were measured for the ten compounds showing the SmC* phase. The short range of the monotropic SmC* phase of compound **Br-1** made it impossible for Ps to be measured.

X-ray measurements were carried out in the SmC* phases in order to determine the tilt angle. Magnetically oriented diffraction patterns were obtained by aligning the SmA mesophase under a magnetic field of 1.7 T and slow cooling into the SmC* mesophase. The interlayer spacing in the SmA and SmC* phases was calculated from the measured low-angle diffraction maxima (2θ = 2.8–2.9°). The data obtained indicate that in the SmC* mesophase, the layer thickness is only slightly smaller (1 or 2 Å at most) than in the SmA mesophase and decreases gradually on decreasing the temperature. By comparing the layer thickness in the SmA and SmC* phases, a maximum value for the tilt angle in the SmC* phase between 15° and 18° can be estimated.

All the data related to the ferroelectric properties of the nine evaluated compounds are gathered in Table II: Ps max values, Ps values at $T-T_c$ = −10 °C, and response times calculated from

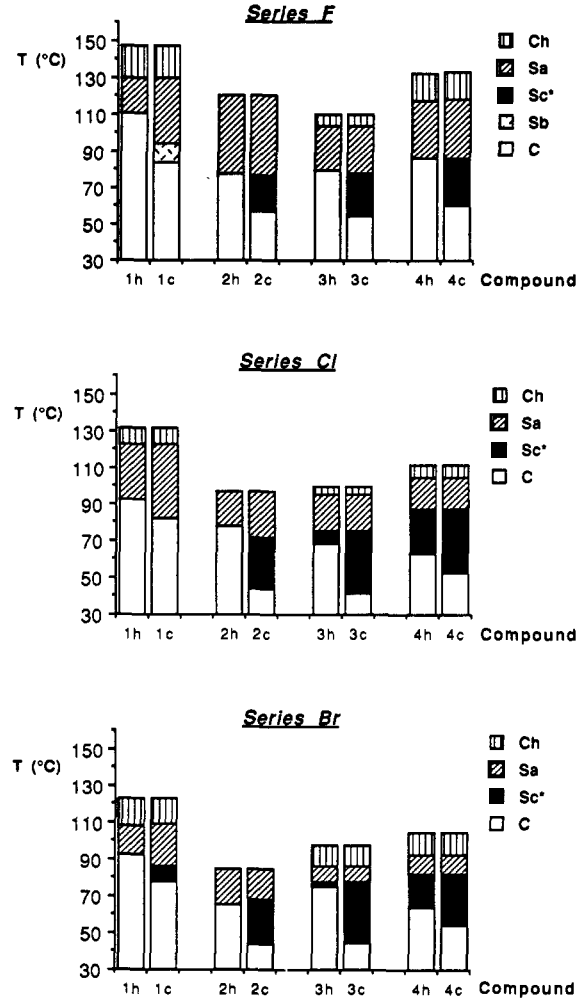

Figure 1. Mesophase ranges of the compounds in series **F**, **Cl**, and **Br** in the heating (h) and cooling (c) processes.

Table II. Spontaneous Polarization (Ps max and Ps ($T-T_c$ = −10°)) and Response Times (τE) Values Measured for the Nine Compounds Showing the SmC* Mesophase

compound	Ps max (nC/cm²)	Ps[a] (nC/cm²)	τE[a] (μsV/μm)
F-2	−16	−15	55
F-3	−102	−85	109
F-4	−85	−62	100
Cl-2	−47	−41	144
Cl-3	−100	−70	110
Cl-4	−95	−57	81
Br-1	−30	−29	152
Br-3	−66	−50	183
Br-4	−59	−46	156

[a] Data measured at $T-T_c$ = −10 °C.

(17) Gray, G. W. *Thermotropic Liquid Crystals*; Biddles Ltd., UK, 1987.
(18) Coates, D. *Liquid Crystals* **1987**, *2*, 63.
(19) Matsumoto, S.; Hatoh, H.; Kamagami, S.; Muruyama, A. *Ferroelectrics* **1988**, *85*, 235.

Table III. Abundance, Dihedral Angles, and Module of the Dipole Moments of the Most Representative Conformations for Each α-Halo Acid Minimized by MM2

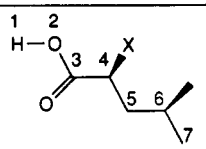
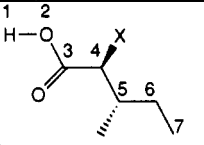
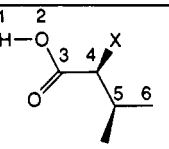

X	%[a]	2-3-4-5[b]	3-4-5-6[b]	4-5-6-7[b]	2-3-4-X[b]	μ[c]	%[a]	2-3-4-5[b]	3-4-5-6[b]	4-5-6-7[b]	2-3-4-X[b]	μ[c]	%[a]	2-3-4-5[b]	3-4-5-6[b]	2-3-4-X[b]	μ[c]
F	48	125.2	−179.6	−62.6	4.1	0.1	44	124.8	−61.6	173.6	2.2	0.1	65	124.1	−61.5	1.8	0.1
Cl	23	113.6	172.0	−61.3	−12.3	0.4	32	129.7	−64.5	170.2	1.0	0.2	31	117.7	−64.6	−10.6	0.3
	22	156.9	174.4	−59.1	30.8	0.9	15	137.4	−75.3	59.0	6.5	0.3	30	128.3	−64.6	−0.2	0.2
Br	30	−160.6	173.5	−60.6	75.1	2.0	15	−172.8	−68.7	164.2	58.4	1.6	25	−142.3	176.4	93.0	2.4
	24	−147.0	58.0	−178.2	89.6	2.3	10	59.2	171.5	176.0	−77.9	1.9	24	59.2	171.7	−67.4	1.8
							10	−139.4	176.3	176.2	95.6	2.5					

[a] Percentage of the corresponding conformation in the conformational population. [b] Torsional angle defined by the atoms whose numbers are indicated in the figure above. [c] Dipole moment of the conformation in Debyes

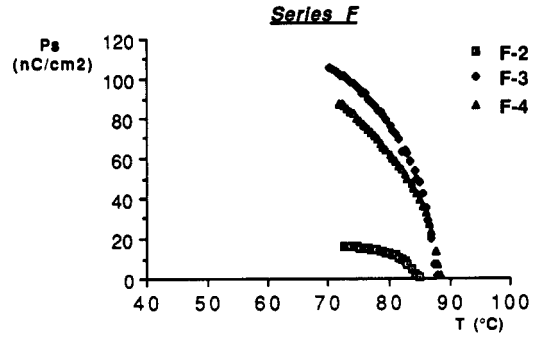

Figure 2. Temperature dependence of the polarization of the compounds in series **F** (**F-2**, **F-3**, and **F-4**) in the SmC* phase.

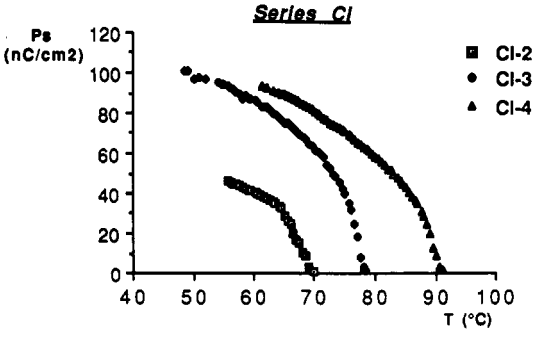

Figure 3. Temperature dependence of the polarization of the compounds in series **Cl** (**Cl-2**, **Cl-3**, and **Cl-4**) in the SmC* phase.

the Ps ($T-T_c = -10$ °C) values using the equation $\tau = k\gamma_c/PsV$[20,21] and given on an applied electric field step E. Optical measurements of all these naphthalene derivatives showed a negative Ps sign as well as a clearly electroclinic effect at the SmA phase, around 10 °C above the SmA–SmC* transition.

Figures 2–4 show the dependence of the spontaneous polarization against the temperature in series **F**, **Cl**, and **Br**, respectively. The increase in the Ps values of all the compounds is gradual when the temperature decreases. The second-order nature of the transition SmA–SmC* was corroborated by differential scanning calorimetry where no peak appeared for this transition in any of the compounds.

MM2 Calculations. The MM2 program allows the calculation of the different conformers of a σ-bond and their relative abundance.[9] In 1989 a modification of this program—MM2PRIME—was published.[22] With the "treecoverage" option, included therein, up to six bonds may be rotated twice every 120°, so that all three staggered rotamers (one anti and two gauche for

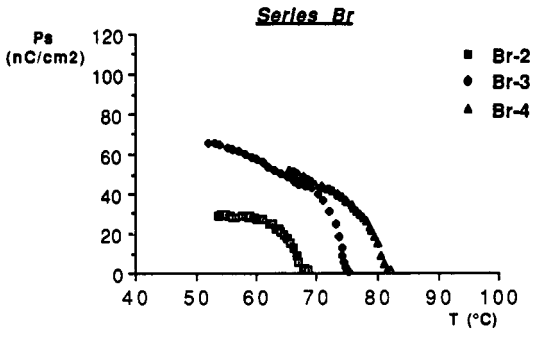

Figure 4. Temperature dependence of the polarization of the compounds in series **Br** (**Br-2**, **Br-3**, and **Br-4**) in the SmC* phase.

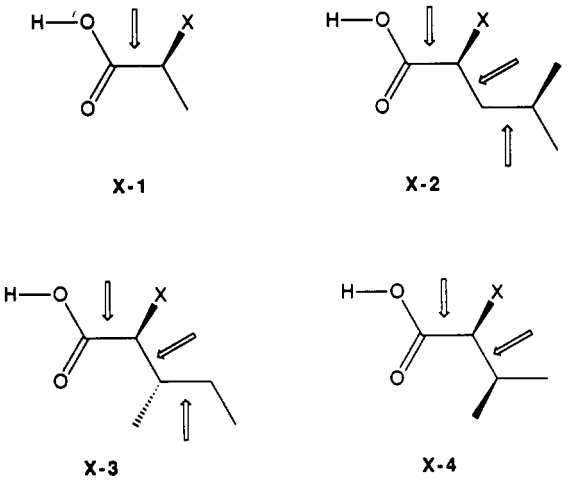

Figure 5. Models minimized by MM2. The bonds marked with an arrow were allowed to rotate during the running of the program.

every rotated σ-bond) can be minimized. This is done automatically for all combinations over the specified bonds. 3^n rotamers are all generated and minimized. Their relative abundance is calculated from the corresponding minima steric energy values.

In order to determine the nature of the influence of the chiral tails on the ferroelectric properties, we have minimized all 12 using the corresponding α-halo acids as models. In these models the rest of the molecule has been substituted by an H atom so that the calculations can be simplified. This H atom has no effect on the conformational study because only the bonds directly involved in the asymmetric part of the molecule were allowed to rotate during the running of the program (see Figure 5).

Data concerning the most representative conformations of each acid are gathered in Table III (only data concerning the acids involved in our discussion are represented, **X-2**, **X-3**, and **X-4**). A study of the global conformational populations for each tail showed that the conformations in Table III are reliable enough to be used in our studies. Our criterion for the representativity

(20) Jiu-Zie, X.; Handshy, M.; Clark, N. A. *Ferroelectrics* **1987**, *73*, 305.
(21) Escher, C.; Geelhaar, T.; Bohm, E. *Liquid Crystals* **1988**, *3*, 469.
(22) Osawa, E.; Jaime, C.; Fujiyoshi, T.; Goto, H.; Imai, K. *J.C.P.E. Newsletter* **1989**, *1*, Program No. 9 (backsversion).

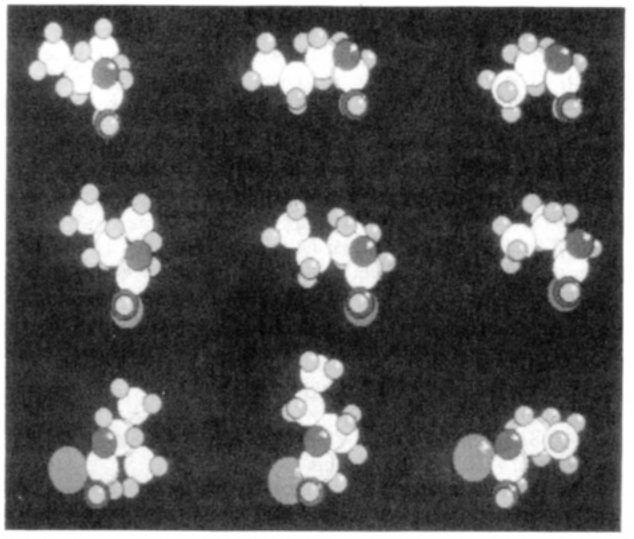

Figure 6. Graphical representation of the most abundant conformation for each minimized α-halo acid, L-leucine, L-isoleucine, and L-valine derivatives.

of each conformation depended on whether its percentage was considerably higher than that of the next most abundant conformation. On this basis, we selected one conformation for every component in series **F** and two conformations for every component in series **Cl** and for **Br-2** and **Br-4** in series **Br**. In the eight cases approximately 50% of the total conformational population is represented. The α-bromo acid derived from isoleucine (**Br-3**) was a more difficult case when it came to choosing the most representative conformations because of a more equal distribution of abundances. In this compound, we picked out the three conformations with the highest percentages, even though they represent only 35% of the total population.

In order to have graphical support for our discussion of the molecular structure–ferroelectric properties relationship, Figure 6 shows each of these minimized acids. For the sake of simplification, only the most abundant conformation of each tail has been graphically represented.

Molecular Structure–Ferroelectric Properties. With regard to the alkyl group in the chiral center, a clear tendency is deduced in each series from observation of the experimental Ps values: The presence of an isoleucine derivative as a chiral tail gives rise to the highest Ps values. The lowest values belong to the leucine-derived chiral tails.

In Table III we can observe a clear difference between the conformations of leucine and the isoleucine and valine derivatives. The dihedral angle defined by the atoms 3-4-5-6 gives rise to very different conformations for the alkyl groups in the asymmetric center (*C4). In leucine derivatives (X = F, Cl, Br) this group keeps, in general, the linearity of the tail with dihedral angles close to the anti position (173–179°). On the other hand, the bulky group is situated on the outside of the anti–anti conformation of the skeleton of the chiral tail in L-isoleucine and L-valine derivatives showing 3-4-5-6 dihedral angles of between 61° and 70°. Taking all these data into account and observing Figure 6, we can understand how these tails can influence the ferroelectric properties of their corresponding compounds: it is obvious that the steric hindrance produced by the tails derived from isoleucine which affects the free independent rotation of the molecules around their long axes is the major cause of their higher Ps values; a better intermolecular coupling of the C–X dipoles is favored. Slightly lower Ps values were measured for valine derivatives, which show a less bulky ramification adjacent to the asymmetric center. In leucine derivatives, the previously mentioned linearity allows more easily the unfavorable independent rotation.

With regard to the different halogen atom in the chiral carbon, we can observe in Table II, with the exception of **F-2**, a decrease in the Ps ($T - T_c = -10$ °C) values on the sequence F > Cl > Br, specially marked when going from Cl to Br.

The incorporation of a strong dipole moment into the asymmetric center is known to give rise to high Ps values.[23-25] Given the small differences in the modules of the dipole moments of the three C–X bonds, μC–F = 1.41 D, μC–Cl = 1.44 D, μC–Br = 1.38 D, such considerable differences in the Ps values were not to be expected. There must therefore be a strong steric factor which influences the way these dipoles interact in the SmC* layer.

In Table III, we can observe that the dihedral angle corresponding to the agrupation O–CO–*C–X increases from 0° to almost 90° as the halogen atom is bigger. This fact has two opposite effects as far as the Ps values are concerned. On the one hand, as the dihedral angle moves away from 0°, the C → X dipole is more coupled to the dipole of the ester group and the module of the molecular dipole increases, with a sequence Br > Cl > F. On the other hand, as the dihedral angle increases, the halogen atom moves away from the plane defined by the ester group; this greatly influences the molecular arrangement as will be shown below.

These preliminary conclusions lead us to think that not only the magnitude of the dipoles in the chiral tail is responsible for the Ps values. Even more important than this is the way these dipoles interact sterically with those of contiguous molecules.

In order to define this steric intermolecular interaction, we must consider the steric requirements of the halogen atom with regard to those of the bulky alkyl group in the asymmetric center. As can be observed in Figure 6, the smaller the halogen atom, the more protected it is by the alkyl group. This allows the molecules to come closer to each other and the asymmetric parts to interact in such a way that the independent mobility of the molecules around their long axes is more hindered. At this point, it can be said that in the compounds of series **F** and **Cl**, the alkyl group is directly responsible for molecular arrangement and consequently responsible for the higher Ps values: the more asymmetric parts of the contiguous molecules interact, the stronger the dipolar coupling is; the dipolar density in the SmC* layer increases and so does Ps. Furthermore, the homogeneity of the conformational population (dihedral angles) in the compounds of series **F** and **Cl** (see Table III) facilitate this favorable intermolecular interaction.

In the compounds of series **Br**, we can observe a drastic change in the shape of the chiral tails. Now, the positive effect that the ramification of the alkyl groups had in series **F** and **Cl** is annulled, on the one hand, by the leadership of the bromine atom in the molecular arrangement: the dipolar density is much smaller giving rise to lower Ps values, and, on the other hand, by the strong differences in the most representative conformations for each tail (see Table III) which makes adequate steric intermolecular interactions difficult.

As far as the response times are concerned, no clear tendency is observed from the data in Table II. What we do deduce is the much lower viscosity of compounds containing fluorine or chlorine atoms in their chiral tails, showing response times, in the order of 10 μs for an applied electric field of ±10 V/μm.

Conclusion

Three new series of FLC compounds, with F, Cl, or Br in their chiral center, have been prepared. Compounds with chiral tails bearing a small halogen atom (as F or Cl) and a ramificated bulky alkyl group in its chiral center show the highest Ps values, i.e., **F-3**, 2′-[6′-((2″*S*,3″*S*-2″-fluoro-3″-methylpentanoyl)oxy)]naphthyl 4-decyloxybenzoate, Ps = 102 nC/cm², and **Cl-3**, 2′-[6′-((2″*S*,3″*S*-2″-chloro-3″-methylpentanoyl)oxy)]naphthyl 4-decyloxybenzoate, Ps = 100 nC/cm². MM2 calculations show

(23) Tinh, N. H.; Salleneuve, C.; Babeau, A.; Galvan, J. M.; Destrade, C. *Mol. Cryst. Liq. Cryst.* **1987**, *151*, 147.
(24) Bahr, Ch.; Heppke, G. *Mol. Cryst. Liq. Cryst.* **1987**, *148*, 29.
(25) Sakurai, T.; Mikami, N.; Higuchi, R.; Honma, M.; Yoshino, K. *Ferroelectrics* **1988**, *85*, 469.
(26) Pérez-Jubindo, M. A.; Tello, M. J.; Fernández, J. *J. Phys. D.* **1981**, *14*, 2305.
(27) Miyasato, K.; Abe, S.; Takezoe, H.; Fukuda, A.; Kuze, E. *Jpn. J. Appl. Phys.* **1983**, *22*, L661.
(28) De la Fuente, M. R.; Ezcurra, A.; Pérez-Jubindo, M. A.; Zubía, J. *Liquid Crystals* **1990**, *7*, 51.

that the steric factors of the chiral tail have a decisive influence on the ferroelectric properties by controlling the molecular arrangement within the SmC* phase and the intermolecular interactions of the molecular dipoles. This paper shows how empirical calculations can be successfully used to understand the influence of structural factors on ferroelectric behavior; which will allow us to design high spontaneous polarization FLC compounds in further studies.

Experimental Section

Synthesis. Representative Procedure for Obtaining (*S*)-α-Fluorocarboxylic Acids [2]. 2*S*-2-Fluoro-4-methylpentanoic acid (2, R = $CH_2CH(CH_3)_2$, X = F). A polypropylene flask equipped with a stirring bar was charged with 3.93 g (0.03 mol) of L-leucine [1] and 45 mL of commercial HF/Py [70/30]. The reaction mixture was cooled with an ice/water bath, and, with vigorous stirring, 3.66 g (0.053 mol) of $NaNO_2$ was added in small portions for 1 h. Stirring was continued at room temperature for 6 h longer. The reaction mixture was quenched with 100 mL of ice/water. The solution was extracted with diethyl ether (4 times 100 mL). The combined organic layers were washed twice with brine and dried over $MgSO_4$. The solvent was removed under vacuum, and the crude was twice distilled to afford 1.6 g of 2*S*-2-fluoro-4-methylpentanoic acid: yield 40%; bp 115 °C, 15 mmHg; ^1H NMR ($CDCl_3$) δ 0.9 (d, 6 H, J = 6 Hz), 1.3–1.7 (m, 1 H), 1.8 (dm, 2 H, J_{FH} = 28 Hz), 4.2 (ddd, 1 H, J_{FH} = 48 Hz, J_1 = 9 Hz, J_2 = 8.5 Hz), 10.6 (s, 1 H); IR (neat) 3500–2500, 1744 cm^{-1}.

2*S*,3*S*-2-Fluoro-3-methylpentanoic Acid [2, R = –*CH(CH$_3$)CH$_2$CH$_3$, X = F]. A polypropylene flask equipped with a stirring bar was charged with 3.93 g (0.03 mol) of L-isoleucine [1] and 21.6 mL of dry pyridine. The mixture was cooled with an ice/water bath, and then 50.4 mL of commercial HF/Py [70/30] was slowly added. To this reaction mixture was added 3.66 g (0.053 mol) of $NaNO_2$ in small portions of 1 h. Stirring was continued at room temperature for 5 h longer. The workup and purification were as described for the previous *S*-α-fluorocarboxylic acid, affording 0.4 g of the pure 2*S*,3*S*-2-fluoro-3-methylpentanoic acid: yield 10%; bp 75 °C, 3 mmHg; ^1H NMR ($CDCl_3$) δ 1.0 (t, 3 H, J = 7 Hz), 1.2 (d, 3 H, J = 7 Hz), 1.3 (m, 2 H), 2.1 (dm, 1 H, J_{FH} = 24 Hz), 4.8 (dd, 1 H, J_{FH} = 48 Hz, J = 7 Hz), 10.6 (s, 1 H); IR (neat) 3500–2500, 1730 cm^{-1}.

Analytical Data for Other Compounds 2 (X = F). 2*S*-2-Fluoropropanoic Acid [2, R = –CH$_3$, X = F]. Bp 90 °C, 15 mmHg; ^1H NMR ($CDCl_3$) δ 1.5 (dd, 3 H, J_{FH} = 24 Hz, J = 7 Hz), 4.3 (dc, 1 H, J_{FH} = 48 Hz, J = 7 Hz), 10.3 (s, 1 H); IR (neat) 3500–2500, 1734 cm^{-1}. **2*S*-2-Fluoro-3-methylbutanoic Acid [2, R = –CH(CH$_3$)$_2$, X = F].** Bp 96 °C, 15 mmHg; ^1H NMR ($CDCl_3$) δ 1.0 (d, 3 H, J = 6 Hz), 1.1 (d, 3 H, J = 6 Hz), 1.3–1.7 (dm, 1 H, J_{FH} = 24 Hz), 4.2 (dd, 1 H, J_{FH} = 48 Hz, J = 7 Hz), 10.6 (s, 1 H); IR (neat) 3500–2500, 1744 cm^{-1}.

Representative Procedure for Obtaining *S*-α-Chlorocarboxylic Acids [2]. 2*S*,3*S*-2-Chloro-3-methylpentanoic Acid [2, R = –*CH(CH$_3$)CH$_2$CH$_3$, X = Cl]. A flask equipped with a stirring bar was charged with 7.86 g (0.06 mol) of L-isoleucine [1] and 75 mL of 6 N HCl. The reaction mixture was cooled with an ice/water bath, and, with vigorous stirring, $NaNO_2$ (6.62 g, 0.096 mol) was added in small portions of 1 h. Stirring was continued at 0 °C for 4 h longer. The solution was extracted four times with 150-mL portions of diethyl ether. The combined organic layers were extracted twice with brine and dried over $MgSO_4$. The solvent was removed under vacuum, and the crude was twice distilled to afford 4.4 g of 2*S*,3*S*-2-chloro-3-methylpentanoic acid: yield 40%; bp 125 °C, 15 mmHg; ^1H NMR ($CDCl_3$) δ 0.9 (t, 3 H, J = 8 Hz), 1.1 (d, 3 H, J = 7 Hz), 1.5 (m, 2 H), 2.1 (m, 1 H), 4.3 (d, 1 H, J = 7 Hz), 10.5 (s, 1 H); IR (neat) 3600–2400, 1722 cm^{-1}.

Analytical Data for Other Compounds 2 (X = Cl). 2*S*-2-Chloropropanoic Acid [2, R = –CH$_3$, X = Cl]. Bp 180 °C, 760 mmHg; ^1H NMR ($CDCl_3$) δ 1.6 (d, 3 H, J = 7 Hz), 4.3 (c, 1 H, J = 7 Hz), 9.8 (s, 1 H); IR (neat) 3600–2400, 1724 cm^{-1}. **2*S*-2-Chloro-4-methylpentanoic Acid [2, R = –CH$_2$CH(CH$_3$)$_2$, X = Cl].** Bp 79 °C, 3 mmHg; ^1H NMR ($CDCl_3$) δ 0.9 (d, 3 H, J = 6.5 Hz), 1.0 (d, 3 H, J = 6.5 Hz), 1.3–1.7 (m, 1 H), 1.8 (m, 2 H), 4.2 (t, 1 H, J = 8 Hz), 10.6 (s, 1 H); IR (neat) 3500–2500, 1725 cm^{-1}.

2*S*-2-Chloro-3-Methylbutanoic Acid [2, R = –CH(CH$_3$)$_2$, X = Cl]. Bp 70 °C, 3 mmHg; ^1H NMR ($CDCl_3$) δ 1.0 (d, 6 H, J = 7 Hz), 2.3 (m, 1 H), 4.2 (d, 1 H, J = 6 Hz), 9.5 (s, 1 H); IR (neat) 3700–2500, 1722 cm^{-1}.

Representative Procedure for Obtaining *S*-α-Bromocarboxylic Acids [2]. 2*S*,3*S*-2-Bromo-3-methylpentanoic Acid [2, R = –*CH(CH$_3$)CH$_2$CH$_3$, X = Br]. A flask equipped with a stirring bar was charged with 7.86 g (0.06 mol) of L-isoleucine [1] and 75 mL of 6 N HBr. The reaction mixture was cooled with an ice/water bath, and, with vigorous stirring, $NaNO_2$ (6.62 g, 0.096 mol) was added in small portions for 1 h. Stirring was continued at 0 °C for 4 h longer. The solution was extracted four times with 150-mL portions of diethyl ether. The combined organic layers were extracted twice with brine and dried over $MgSO_4$. The solvent was removed under vacuum, and the crude was twice distilled to afford 2.8 g of 2*S*,3*S*-2-bromo-3-methylpentanoic acid: yield 24%; bp 100 °C, 3 mmHg; ^1H NMR ($CDCl_3$) δ 1.0 (t, 3 H, J = 7.5 Hz), 1.1 (d, 3 H, J = 7 Hz), 1.3–2.3 (m, 3 H), 4.1 (d, 1 H, J = 7 Hz), 10.9 (s, 1 H); IR (neat) 3600–2400, 1716 cm^{-1}.

Analytical Data for Other Compounds 2 (X = Br). 2*S*-2-Bromopropanoic Acid [2, R = –CH$_3$, X = Br]. Bp 45 °C, 3 mmHg; ^1H NMR ($CDCl_3$) δ 1.8 (d, 3 H, J = 7 Hz), 4.4 (c, 1 H, J = 7 Hz), 11.4 (s, 1 H); IR (neat) 3500–2500, 1722 cm^{-1}. **2*S*-2-Chloro-4-methylpentanoic Acid [2, R = –CH$_2$CH(CH$_3$)$_2$, X = Br].** Bp 145 °C, 15 mmHg; ^1H NMR ($CDCl_3$) δ 0.9 (d, 3 H, J = 7 Hz), 1.1 (d, 3 H, J = 7 Hz), 1.3–1.7 (m, 1 H), 1.9 (m, 2 H), 4.3 (t, 1 H, J = 7.5 Hz), 10.4 (s, 1 H); IR (neat) 3600–2500, 1714 cm^{-1}.

2*S*-2-Chloro-3-methylbutanoic Acid [2, R = –CH(CH$_3$)$_2$, X = Br]. Bp 85 °C, 3 mmHg; ^1H NMR ($CDCl_3$) δ 1.0 (d, 3 H, J = 6 Hz), 1.1 (d, 3 H, J = 6 Hz), 2.0–2.4 (m, 1 H), 4.1 (d, 1 H, J = 8 Hz)), 10.9 (s, 1 H); IR (neat) 3600–2400, 1715 cm^{-1}.

2′-(6′-Hydroxy)naphthyl 4-Decyloxybenzoate [6]. To a stirred saturated solution of 2.4 g (15 mmol) of 2,6-dihydroxynaphthalene [4] in dry pyridine, under nitrogen atmosphere, 2.97 g (10 mmol) of 4-decyloxybenzoyl chloride [5] was added dropwise, and the reaction mixture was stirred at room temperature for 24 h. The reaction mixture was quenched with 110 mL of 2 N HCl/ice mixture and stirred for 30 min. The solid was filtered off and washed several times with water. The product was purified by flash chromatography on silica gel with 0.5% hexane/dichloromethane as an eluent to afford 1.68 g of a slightly yellow solid: yield 40%. For further purification the product was recrystallized from ethanol: C 136.0 °C N 148.5 °C I; ^1H NMR ($CDCl_3$) δ 0.89 (t, 3 H), 1.28–1.48 (m, 14 H), 1.81–1.85 (m, 2 H), 4.05 (t, 2 H), 6.04 (s, 1 H), 6.99 (d, 2 H, J_o = 9 Hz), 7.04 (m, 2 H), 7.25 (dd, 1 H, J_o = 8.5 Hz, J_m = 1.5 Hz), 7.55 (d, 1 H, J_m = 2.1 Hz), 7.60 (d, 1 H, J_o = 8.6 Hz), 7.61 (d, 1 H, J_o = 8.3 Hz), 8.20 (d, 2 H, J_o = 9 Hz); IR (neat) 3602, 1697, 1605, 1510, 1462, 1260 cm^{-1}.

Representative Procedure for Coupling of 2′-(6′-Hydroxy)naphthyl 4-Decyloxybenzoate [6] with (*S*)-α-Haloacyl Chlorides [7]. 2′-[6′-((2″*S*,3″*S*-2″-fluoro-3″-methylpentanoyl)oxy)]naphthyl 4-Decyloxybenzoate [7, R = –*CH(CH$_3$)CH$_2$CH$_3$, X = F]. (a) A mixture of 151.4 mg (1.13 mmol) of 2*S*,3*S*-2-fluoro-3-methylpentanoic acid [2], 0.6 mL of Cl_2SO, and 0.6 mL of dry benzene was refluxed until no evolution of HCl gas was detected. The benzene and the excess of Cl_2SO were removed by evaporation. The liquid residue was used in the next step without further purification. (b) To a stirred solution of 474.6 mg (1.13 mmol) of 2′-(6′-hydroxy)naphthyl 4-decyloxybenzoate and 114.3 mg (1.13 mmol) of triethylamine in 20 mL of dry chloroform was added dropwise via syringe a solution of 172.3 mg (1.13 mmol) of 2*S*,3*S*-2-chloro-3-methylpentanoyl chloride in 5 mL of chloroform. The reaction mixture was stirred for 5 h at room temperature. The solvent was removed under vacuum, and the product was purified by flash chromatography with 30% hexane/toluene as eluent. The pure product was twice recrystallized from ethanol and hexane: yield 79%; ^1H NMR (300 MHz, $CDCl_3$) δ 0.89 (t, 3 H), 1.04 (t, 3 H, J = 7.4 Hz), 1.18 (d, 3 H, J = 6.8), 1.29 (m, 2 H), 1.30–1.80 (m, 17 H), 2.10 (dm, 1 H, J_{FH} = 24.0 Hz), 4.06 (t, 2 H, J = 6.3 Hz), 5.06 (dd, 1 H, J_{FH} = 48.6 Hz, J = 4.5 Hz), 6.98 (d, 2 H, J = 9.0 Hz), 7.26 (dd, 1 H, J_o = 9.0 Hz, J_m = 2.0 Hz), 7.38 (dd, 1 H, J_o = 8.8 Hz, J_m = 2.2 Hz), 7.61 (d, 1 H, J_m = 2.0 Hz), 7.68 (d, 1 H, J_m = 2.2 Hz), 7.85 (d, 1 H, J_o = 9.0 Hz), 7.86 (d, 1 H, J_o = 8.8 Hz), 8.17 (d, 2 H, J = 9.0 Hz); IR (Nujol) 1774, 1729, 1607, 1512, 1270, 1070 cm^{-1}; UV–vis λ (log ε) 223 (4.67), 261 (4.55), 267 sh. Anal. Calcd for $C_{33}H_{41}O_5F$: C, 73.88; H, 7.65. Found: C, 74.27; H, 8.04.

Analytical Data of Other Compounds 7. 2′-[6′-(2″*S*-2″-Fluoropropanoyloxy)]naphthyl 4-Decyloxybenzoate [7, R = –CH$_3$, X = F]. ^1H NMR (300 MHz, $CDCl_3$) δ 0.89 (t, 3 H), 1.30–1.80 (m, 17 H), 1.80 (dd, 3 H, J_{FH} = 29.5 Hz, J = 6.9 Hz), 4.06 (t, 2 H, J = 6.3 Hz), 5.32 (dc, 1 H, J_{FH} = 48.4 Hz, J = 6.9 Hz), 6.98 (d, 2 H, J = 9.0 Hz), 7.26 (dd, 1 H, J_o = 9.0 Hz, J_m = 2.0 Hz), 7.38 (dd, 1 H, J_o = 8.8 Hz, J_m = 2.2 Hz), 7.61 (d, 1 H, J_m = 2.0 Hz), 7.68 (d, 1 H, J_m = 2.2 Hz), 7.85 (d, 1 H, J_o = 9.0 Hz), 7.86 (d, 1 H, J_o = 8.8 Hz), 8.17 (d, 2 H, J = 9.0 Hz); IR (Nujol) 1775, 1729, 1608, 1512, 1280, 1071 cm^{-1}; UV–vis λ (log ε) 223 (4.68), 261 (4.55), 265 sh. Anal. Calcd for $C_{30}H_{35}O_5F$: C, 72.87; H, 7.09. Found: C, 73.05; H, 7.80.

2′-[6′-((2″*S*-2″-Fluoro-4″-methylpentanoyl)oxy)]naphthyl 4-Decyloxybenzoate [7, R = –CH$_2$CH(CH$_3$)$_2$, X = F]. ^1H NMR (300 MHz, $CDCl_3$) δ 0.89 (t, 3 H), 1.07 (d, 6 H, J = 5.9 Hz), 1.28 (m, 1 H), 1.90 (dm, 2 H, J_{FH} = 30.0 Hz), 1.30–1.80 (m, 17 H), 4.06 (t, 2 H, J = 6.3 Hz), 5.24 (ddd, 1 H, J_{FH} = 50.0 Hz, J_1 = 9.2 Hz, J_2 = 8.5 Hz), 6.98 (d, 2 H, J = 9.0 Hz), 7.26 (dd, 1 H, J_o = 9.0 Hz, J_m = 2.0 Hz), 7.38

(dd, 1 H, J_o = 8.8 Hz, J_m = 2.2 Hz), 7.61 (d, 1 H, J_m = 2.0 Hz), 7.68 (d, 1 H, J_m = 2.2 Hz), 7.85 (d, 1 H, J_o = 9.0 Hz), 7.86 (d, 1 H, J_o = 8.8 Hz), 8.17 (d, 2 H, J = 9.0 Hz); IR (Nujol) 1777, 1724, 1607, 1511, 1272, 1072 cm^{-1}; UV–vis λ (log ε) 224 (4.69), 261 (4.55), 267 sh. Anal. Calcd for $C_{33}H_{41}O_5F$: C, 73.88; H, 7.65. Found: C, 73.86; H, 8.04.

2′-[6′-((2″*S*-2″-fluoro-3″-methylbutanoyl)oxy)]naphthyl 4-Decyloxybenzoate [7, R = –CH(CH$_3$)$_2$, X = F]. ^{1}H NMR (300 MHz, $CDCl_3$) δ 0.89 (t, 3 H), 1.16 (d, 3 H, J = 7.0 Hz), 1.21 (d, 3 H, J = 7.1 Hz), 1.30–1.80 (m, 17 H), 2.50 (dm, 1 H, J_{FH} = 22.0 Hz), 4.06 (t, 2 H, J = 6.3 Hz), 5.00 (dd, 1 H, J_{FH} = 45.2 Hz, J = 4.1 Hz), 6.98 (d, 2 H, J = 9.0 Hz), 7.26 (dd, 1 H, J_o = 9.0 Hz, J_m = 2.0 Hz), 7.38 (dd, 1 H, J_o = 8.8 Hz, J_m = 2.2 Hz), 7.61 (d, 1 H, J_m = 2.0 Hz), 7.68 (d, 1 H, J_m = 2.2 Hz), 7.85 (d, 1 H, J_o = 9.0 Hz), 7.86 (d, 1 H, J_o = 8.8 Hz), 8.17 (d, 2 H, J = 9.0 Hz); IR (Nujol) 1776, 1730, 1606, 1512, 1271, 1072 cm^{-1}; UV–vis λ (log ε) 223 (4.67), 261 (4.55), 266 sh. Anal. Calcd for $C_{32}H_{39}O_5F$: C, 73.56; H, 7.47. Found: C, 74.14; H, 8.18.

2′-[6′-((2″*S*-2″-Chloropropanoyl)oxy)]naphthyl 4-Decyloxybenzoate [7, R = –CH$_3$, X = Cl]. ^{1}H NMR (300 MHz, $CDCl_3$) δ 0.89 (t, 3 H), 1.30–1.80 (m, 17 H), 1.88 (d, 3 H, J = 6.9 Hz), 4.06 (t, 2 H, J = 6.3 Hz), 4.68 (c, 1 H, J = 6.9 Hz), 6.98 (d, 2 H, J = 9.0 Hz), 7.26 (dd, 1 H, J_o = 9.0 Hz, J_m = 2.0 Hz), 7.38 (dd, 1 H, J_o = 8.8 Hz, J_m = 2.2 Hz), 7.61 (d, 1 H, J_m = 2.0 Hz), 7.68 (d, 1 H, J_m = 2.2 Hz), 7.85 (d, 1 H, J_o = 9.0 Hz), 7.86 (d, 1 H, J_o = 8.8 Hz), 8.17 (d, 2 H, J = 9.0 Hz); IR (Nujol) 1756, 1729, 1604, 1510, 1257, 1078 cm^{-1}; UV–vis λ (log ε) 223 (4.66), 261 (4.55), 267 sh. Anal. Calcd for $C_{30}H_{35}O_5Cl$: C, 70.52; H, 6.86. Found: C, 69.94; H, 7.22.

2′-[6′-((2″*S*-2″-Chloro-4″-methylpentanoyl)oxy)]naphthyl 4-Decyloxybenzoate [7, R = –CH$_2$CH(CH$_3$)$_2$, X = Cl]. ^{1}H NMR (300 MHz, $CDCl_3$) δ 0.89 (t, 3 H), 1.04 (d, 3 H, J = 6.4 Hz), 1.05 (d, 3 H, J = 6.3 Hz), 1.29 (m, 1 H), 1.30–1.80 (m, 17 H), 2.03 (m, 2 H), 4.06 (t, 2 H, J = 6.3 Hz), 4.59 (t, 1 H, J = 7.4 Hz), 6.98 (d, 2 H, J = 9.0 Hz), 7.26 (dd, 1 H, J_o = 9.0 Hz, J_m = 2.0 Hz), 7.38 (dd, 1 H, J_o = 8.8 Hz, J_m = 2.2 Hz), 7.61 (d, 1 H, J_m = 2.0 Hz), 7.68 (d, 1 H, J_m = 2.2 Hz), 7.85 (d, 1 H, J_o = 9.0 Hz), 7.86 (d, 1 H, J_o = 8.8 Hz), 8.17 (d, 2 H, J = 9.0 Hz); IR (Nujol) 1768, 1730, 1607, 1513, 1268, 1070 cm^{-1}; UV–vis λ (log ε) 225 (4.71), 270 (4.78). Anal. Calcd for $C_{33}H_{41}O_5Cl$: C, 71.67; H, 7.42. Found: C, 71.90; H, 7.83.

2′-[6′-((2″*S*,3″*S*-2″-chloro-3″-methylpentanoyl)oxy)]naphthyl 4-Decyloxybenzoate [7, R = –*CH(CH$_3$)CH$_2$CH$_3$, X = Cl]. ^{1}H NMR (300 MHz, $CDCl_3$) δ 0.89 (t, 3 H), 1.01 (d, 3 H, J = 8.0 Hz), 1.17 (d, 3 H, J = 6.8 Hz), 1.28 (m, 2 H), 1.30–1.80 (m, 17 H), 2.25 (m, 1 H), 4.06 (t, 2 H, J = 6.3 Hz), 4.42 (d, 1 H, J = 6.9 Hz), 6.98 (d, 2 H, J = 9.0 Hz), 7.26 (dd, 1 H, J_o = 9.0 Hz, J_m = 2.0 Hz), 7.38 (dd, 1 H, J_o = 8.8 Hz, J_m = 2.2 Hz), 7.61 (d, 1 H, J_m = 2.0 Hz), 7.68 (d, 1 H, J_m = 2.2 Hz), 7.85 (d, 1 H, J_o = 9.0 Hz), 7.86 (d, 1 H, J_o = 8.8 Hz), 8.17 (d, 2 H, J = 9.0 Hz); IR (Nujol) 1768, 1730, 1605, 1512, 1269, 1069 cm^{-1}; UV–vis λ (log ε) 223 (4.73), 269 (4.81). Anal. Calcd for $C_{33}H_{41}O_5Cl$: C, 71.67; H, 7.42. Found: C, 71.30; H, 7.75.

2′-[6′-((2″*S*-2″-Chloro-3″-methylbutanoyl)oxy)]naphthyl 4-Decyloxybenzoate [7, R = –CH(CH$_3$)$_2$, X = Cl]. ^{1}H NMR (300 MHz, $CDCl_3$) δ 0.89 (t, 3 H), 1.14 (d, 3 H, J = 6.9 Hz), 1.15 (d, 3 H, J = 6.9 Hz), 1.30–1.80 (m, 17 H), 2.47 (m, 1 H), 4.06 (t, 2 H, J = 6.3 Hz), 4.35 (d, 1 H, J = 6.3 Hz), 6.98 (d, 2 H, J = 9.0 Hz), 7.26 (dd, 1 H, J_o = 9.0 Hz, J_m = 2.0 Hz), 7.38 (dd, 1 H, J_o = 8.8 Hz, J_m = 2.2 Hz), 7.61 (d, 1 H, J_m = 2.0 Hz), 7.68 (d, 1 H, J_m = 2.2 Hz), 7.85 (d, 1 H, J_o = 9.0 Hz), 7.86 (d, 1 H, J_o = 8.8 Hz), 8.17 (d, 2 H, J = 9.0 Hz); IR (Nujol) 1770, 1730, 1608, 1513, 1269, 1070 cm^{-1}; UV–vis λ (log ε) 223 (4.72), 268 (4.81). Anal. Calcd for $C_{32}H_{39}O_5Cl$: C, 71.31; H, 7.24. Found: C, 71.18; H, 7.55.

2′-[6′-((2″*S*-2″-Bromopropanoyl)oxy)]naphthyl 4-Decyloxybenzoate [7, R = –CH$_3$, X = Br]. ^{1}H NMR (300 MHz, $CDCl_3$) δ 0.89 (t, 3 H), 1.30–1.80 (m, 17 H), 1.99 (d, 3 H, J = 6.9 Hz), 4.06 (t, 2 H, J = 6.3 Hz), 4.64 (c, 1 H, J = 6.9 Hz), 6.98 (d, 2 H, J = 9.0 Hz), 7.26 (dd, 1 H, J_o = 9.0 Hz, J_m = 2.0 Hz), 7.38 (dd, 1 H, J_o = 8.8 Hz, J_m = 2.2 Hz), 7.61 (d, 1 H, J_m = 2.0 Hz), 7.68 (d, 1 H, J_m = 2.2 Hz), 7.85 (d, 1 H, J_o = 9.0 Hz), 7.86 (d, 1 H, J_o = 8.8 Hz), 8.17 (d, 2 H, J = 9.0 Hz); IR (Nujol) 1758, 1729, 1608, 1512, 1269, 1069 cm^{-1}; UV–vis λ (log ε) 225 (4.72), 268 (4.79). Anal. Calcd for $C_{30}H_{35}O_5Br$: C, 64.86; H, 6.31. Found: C, 65.26; H. 6.53.

2′-[6′-((2″*S*-2″-Bromo-4″-methylpentanoyl)oxy)]naphthyl 4-Decyloxybenzoate [7, R = –CH$_2$CH(CH$_3$)$_2$, X = Br]. ^{1}H NMR (300 MHz, $CDCl_3$) δ 0.89 (t, 3 H), 1.02 (d, 3 H, J = 6.5 Hz), 1.05 (d, 3 H, J = 6.6 Hz), 1.28 (m, 1 H), 1.30–1.80 (m, 17 H), 2.05 (m, 2 H), 4.06 (t, 2 H, J = 6.3 Hz), 4.54 (t, 1 H, J = 7.6 Hz), 6.98 (d, 2 H, J = 9.0 Hz), 7.26 (dd, 1 H, J_o = 9.0 Hz, J_m = 2.0 Hz), 7.38 (dd, 1 H, J_o = 8.8 Hz, J_m = 2.2 Hz), 7.61 (d, 1 H, J_m = 2.0 Hz), 7.68 (d, 1 H, J_m = 2.2 Hz), 7.85 (d, 1 H, J_o = 9.0 Hz), 7.86 (d, 1 H, J_o = 8.8 Hz), 8.17 (d, 2 H, J = 9.0 Hz); IR (Nujol) 1757, 1731, 1605, 1511, 1274, 1070 cm^{-1}; UV–vis λ (log ε) 223 (4.70), 261 (4.58), 266 sh. Anal. Calcd for $C_{33}H_{41}O_5Br$: C, 66.34; H, 6.87. Found: C, 67.36; H, 7.10.

2′-[6′-((2″*S*,3″*S*-2″-bromo-3″-methylpentanoyl)oxy)]naphthyl 4-Decyloxybenzoate [7, R = –*CH(CH$_3$)CH$_2$CH$_3$, X = Br]. ^{1}H NMR (300 MHz, $CDCl_3$) δ 0.89 (t, 3 H), 1.01 (t, 3 H, J = 7.5 Hz), 1.23 (d, 3 H, J = 6.9 Hz), 1.28 (m, 2 H), 1.30–1.80 (m, 17 H), 2.22 (m, 1 H), 4.06 (t, 2 H, J = 6.3 Hz), 4.38 (d, 1 H, J = 6.9 Hz), 6.98 (d, 2 H, J = 9.0 Hz), 7.26 (dd, 1 H, J_o = 9.0 Hz, J_m = 2.0 Hz), 7.38 (dd, 1 H, J_o = 8.8 Hz, J_m = 2.2 Hz), 7.61 (d, 1 H, J_m = 2.0 Hz), 7.68 (d, 1 H, J_m = 2.2 Hz), 7.85 (d, 1 H, J_o = 9.0 Hz), 7.86 (d, 1 H, J_o = 8.8 Hz), 8.17 (d, 2 H, J = 9.0 Hz); IR (Nujol) 1757, 1725, 1604, 1511, 1261, 1071 cm^{-1}; UV–vis λ (log ε) 222 (4.73), 260 (4.57), 265 sh. Anal. Calcd for $C_{33}H_{41}O_5Br$: C, 66.34; H, 6.87. Found: C, 66.15; H, 6.96.

2′-[6′-((2″*S*-2″-bromo-3″-methylbutanoyl)oxy)]naphthyl 4-Decyloxybenzoate [7, R = –CH(CH$_3$)$_2$, X = Br]. ^{1}H NMR (300 MHz, $CDCl_3$) δ 0.89 (t, 3 H), 1.21 (d, 3 H, J = 6.2 Hz), 1.24 (d, 3 H, J = 6.3 Hz), 1.30–1.80 (m, 17 H), 2.45 (m, 1 H), 4.06 (t, 2 H, J = 6.3 Hz), 4.30 (d, 1 H, J = 7.8 Hz), 6.98 (d, 2 H, J = 9.0 Hz), 7.26 (dd, 1 H, J_o = 9.0 Hz, J_m = 2.0 Hz), 7.38 (dd, 1 H, J_o = 8.8 Hz, J_m = 2.2 Hz), 7.61 (d, 1 H, J_m = 2.0 Hz), 7.68 (d, 1 H, J_m = 2.2 Hz), 7.85 (d, 1 H, J_o = 9.0 Hz), 7.86 (d, 1 H, J_o = 8.8 Hz), 8.17 (d, 2 H, J = 9.0 Hz); IR (Nujol) 1757, 1727, 1603, 1510, 1256, 1070 cm^{-1}; UV–vis λ (log ε) 225 (4.72), 263 (4.58), 268 sh. Anal. Calcd for $C_{33}H_{39}O_5Br$: C, 65.88; H, 6.69. Found: C, 65.78; H, 7.14.

Techniques. Microanalysis was performed with a Perkin-Elmer 240 B microanalyzer. Infrared spectra for all the compounds were obtained by using a Perkin-Elmer 1600 (series FTIR) spectrometer using neat samples for the acid intermediates and Nujol mulls for the final compounds, between polyethylene plates in the 360–4000-cm^{-1} spectral range. The UV–visible spectra for the final compounds were recorded in cyclohexane using a Hitachi V-3400 spectrophotometer in the 200–500-nm spectral range. ^{1}H NMR spectra were recorded on Varian XL-200 and Varian Unity 300 spectrometers operating at 200 and 300 MHz for ^{1}H. The textures of the mesophases were studied with a Nikon optical microscope equipped with a polarizing light, a Mettler FP82 hot stage, and a Mettler FP80 central processor.

Measurements of temperatures of transition were carried out using a Perkin-Elmer DSC-7 differential scanning calorimeter with a heating and cooling rate of 10 °C/min (the apparatus was calibrated with indium, 156.6 °C, and tin, 232.1 °C).

The spontaneous polarization and the response time were obtained simultaneously using the triangular wave form method.[26,27] In the experimental setup[28] the triangular wave voltage is supplied by a HP3325A function generator and then magnified by a KEPCO amplifier. The current-voltage cycles are recorded by a digital acquisition system HP7090A. All the equipment is interfaced to a microcomputer. Cells for measurements are made of two golden-brass electrodes of diameter 12 mm covered with a thin film of polyvinyl alcohol and rubbed in one direction.

Acknowledgment. We thank Dr. J. Barberá, who carried out the X-ray measurements, and Dr. C. Jaime, for his advice on MM2 calculations. This work was financed by the CICYT (Project MAT-88-324-CO2-01).